# Measuring Cell Elasticity of PXE- and TMEM43 cells using an optical stretcher

Daniel Helling
dhelling@physik.uni-bielefeld.de

02.08.2016

# Contents

# Chapter 1

# Declaration of Authorship

I hereby declare that this thesis is my own work and effort and that it has not been submitted anywhere for any award. Where other sources of information have been used, they have been acknowledged.

# Chapter 2

# Motivation

The subject of classical biological analysis is a medium that contains several "identical" cells. This presumption is ultimately untenable, since "identical" cells can show a very heterogeneous appearance. Because of this, there is an increasing demand in tools for single cell analysis.
Biophotonical devices, which are based on the usage of optical forces, are especially useful for this premise: they can catch, move and deform single cells without direct mechanical contact, and they can easily be integrated into further analytical setups. They enable the determination of viscoelastic properties of trapped cells via the deformation of the cytoskeleton. The elasticity or deformability can be affected by several diseases (e.g. cancer, defects in the cell membrane), thus it could serve as a potentially important biomarker.

# Chapter 3

# Theoretical Basics

This part gives a short summary of the fundamental physical principles behind the optical stretcher. Subsequent theoretical explanations can be found in the master thesis of J.Ju [**?**], which provided the basis for this thesis.

## 3.1 Basic principle of the optical stretcher

The idea of using optical scattering and gradient forces was describes first by Arthur Ashkin in 1970 [**?**]. Based on this idea, he developed an optical trap, which is basically a focused beam capable of catching and moving microscopic particles like single cells, plastic beads and even DNA strands. Since then, this setup is typically referred to as optical tweezers.
Based on this idea, Josef Käs and Jochen Guck developed the optical stretcher in the 1990s [1]. It uses two slightly divergent laser beams, which allows for the usage of lower laser powers. This has the advantage of having a lower potential impact on the trapped object, which is preferable especially in live cells. The main advantage compared to optical tweezers is the ability to perform a controlled deformation of trapped objects - depending on their elasticity.
A schematic layout of an optical stretcher is pictured in figure 3.1:

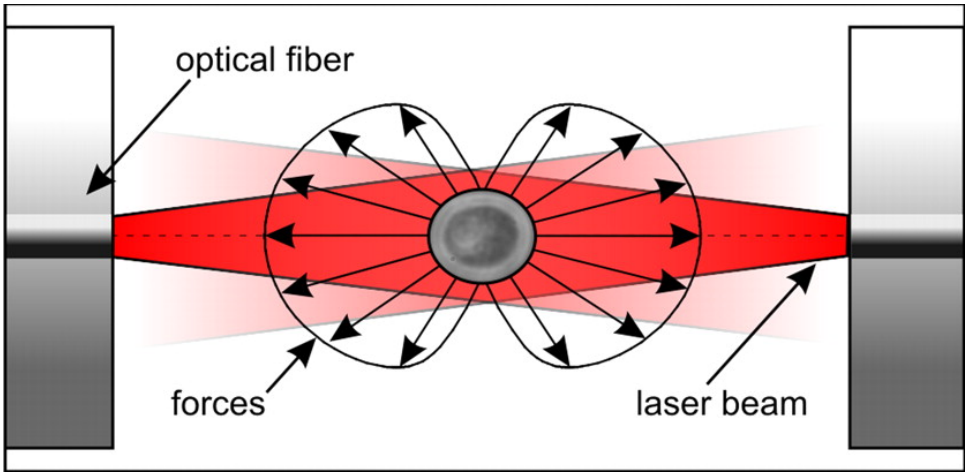


Figure 3.1: schematic layout [2]

When a dielectric particle is being targeted by a slightly divergent laser, it

receives a momentum transfer caused by reflexion. The gradient of the light causes the particle to move to the propagation direction of the optical axis. By using two opposed and slightly divergent lasers, a particle can be trapped. The net sum of the forces that act on the particle equal to zero, but the change in momentum that the laser beam experiences when entering the particle causes a deformation of the particle.
The two laser beams are set to a low laser power, so that a particle in proximity of the optical stretcher will be in a stable position, trapped without deformation. Then the laser power will be increased, and the particle will be stretched along the propagation direction. This process will be recorded by a camera, and the resulting sequence of pictures will be used to determine the deformation.
To understand the actual deformation process more fully, a short overview of the occurring optical forces will be presented in the next chapter. A more detailed overview can be found in [?].

## 3.2 Trap forces

### Geometrical optics

Geometrical optics can be viewed as an edge case of wave optics for small wavelengths. Its main feature is the assumption that light consists of infinitesimal rays of light. The mathematical , but doesn't account for effects such interference and diffraction.

### Wave Optics

### Lorenz-Mie-Theorie

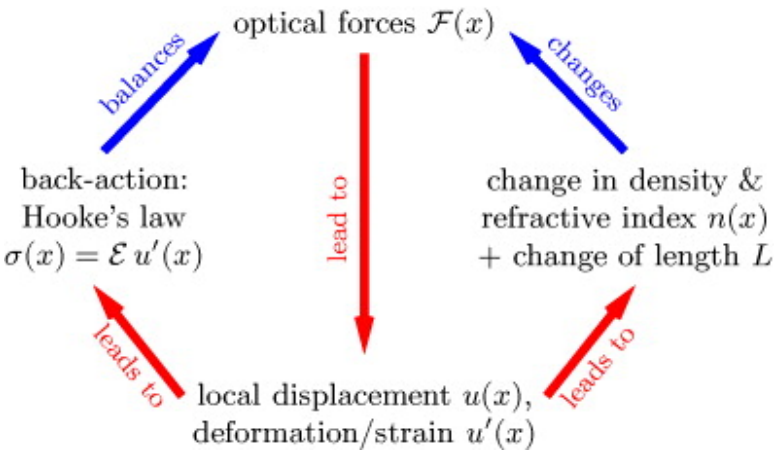


Figure 3.2: Interaction between optical forces and local deformations in elastic medium [3]

## 3.3 Rheology

The images share a resemblance with control circuit and serve the same purpose: To describe the behavior of a system with different dominating elements.

## 3.4 Stretcher designs

A wide variety of designs for the actual setup have been published. Since the alignment of the laser beams is by far the most critical point, these methods typically differ in the actual process of fabricating structures:

- A single droplet of fluid: the easiest method, can be used for experiments that don't require a steady flow of objects
- lithographic processes using PDMS or similar compounds
- glass etching & chemical bonding of two glass plates that contain all the necessary structures
- hybrid designs: often use plus added structures to align the laser fibers

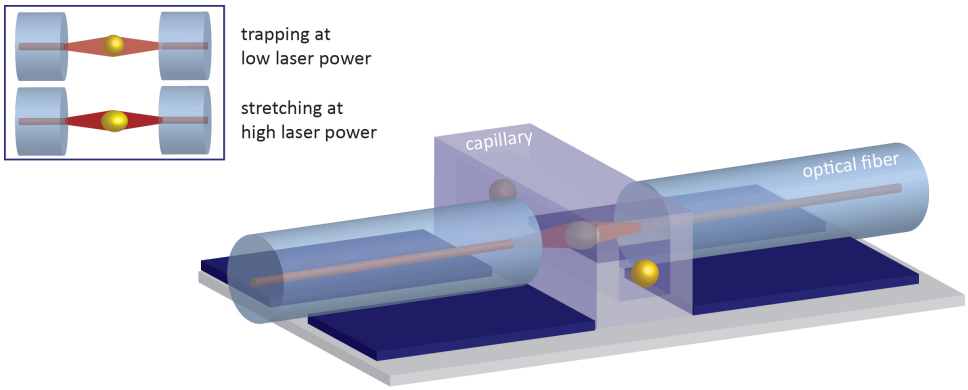


Figure 3.3: hybrid design used in this thesis [**?**]

# Chapter 4

# Biological Basics

This chapter provides a short summary of the biological properties of fibroblasts, which are the cell type used in the following experiments. It also features a basic overview regarding the cell lines used in this work.

## 4.1 Fibroblasts

Fibroblastic cell are a major component of the connective tissue, which is one of the four main types of tissue (including muscular, nerve and epithel tissue). Their main function is maintaing the structural integrity of the connective tissue, which is achieved through the synthesis of intermediate products of the extracellular matrix (the tissue that cells are embedded in). Furthermore, they are responsible for the production of collagen.

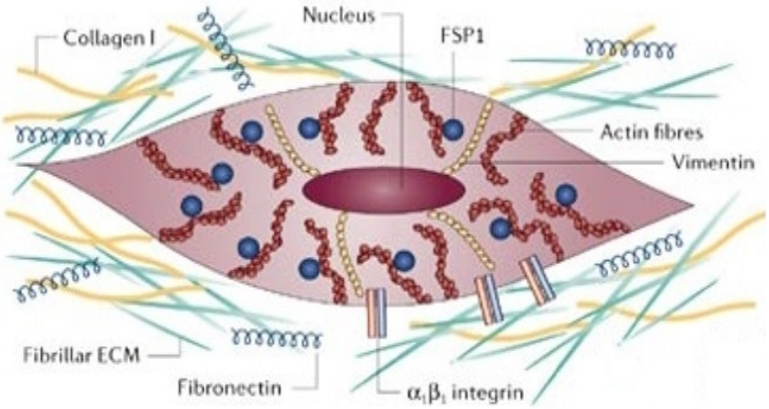


Figure 4.1: general structure of fibroblast cells [**?**]

Fibroblasts also contain stress fibers, which are basically bundles of different proteins (actin and myosin). One end of the stress fiber ends in the plasma membrane of the cell, the other end is either attached to the intermediate filament or

to a different area of the plasma membrane. As the name implies, stress fibers can generate and support tensile forces, allowing the fibroblast to to pull on the extracellular matrix of the connective tissue. [**?**] (ZITAT BOAL CELL MECHANICS) Fibroblasts are very heterogeneous; their appearance depends strongly on their function and localization.

## 4.2 ARVC

ARVC (arrhythmogenic right ventricular cardiomyopathy), also referred to as ARVD (arrhythmogenic right ventricular dysplasia) or ARVD/C (arrhythmogenic right ventricular dysplasia/cardiomyopathy), is an inherited disorder that mainly affects the heart. A genetic defect in the cell membrane of the desmosomes (cell structures that provide the mechanical connection between cells), which are present in the myocardium (heart muscle), causes a replacement of the myocardium by fibrofatty tissue. The exact cause for this behaviour has not been discovered.

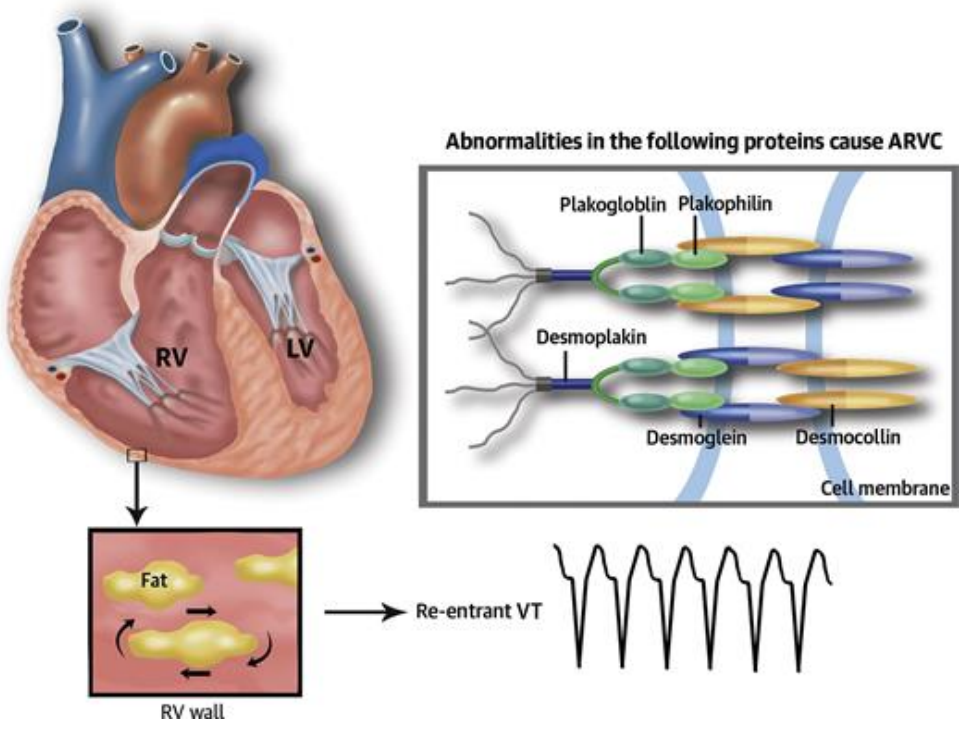


Figure 4.2: Illustration ARVC[**?**]

Since there is a certain phenotypical spectrum to ARVC (morphological changes similar to the ARVC have also been shown in the left ventricle of some patients), it has been suggested that ARVC could be considered as a generalized cardiomyopathy (PAPER RIZZO!!!).
Several genetic mutations in desmosomal proteins have been linked with ARVC, and between 40 and 50 % of patients have been shown to be carriers. One of these mutations is a missense mutation within the gene of transmembrane protein 43 (TMEM43) on chromosome p.S358L (RICHTIG???); cells from patients with this specific mutation were used in the measurements.
ARVC is one of the major causes of cardiac arrhythmias in children and young

adults; it has been suggested that up to 17 % of sudden cardiac deaths in this age group are caused by ARVC. (WIKIPEDIA WOHER???). Predominantly affected are males, who have a lower life expectancy than female carriers. There is no treatment for ARVC itself, but a few treatments are available that aim to manage the disease (including implantable defibrillators and ultimately cardiac transplant surgery).

## 4.3 PXE

PXE (Pseudoxanthoma elasticum), also known as Grönblad-Strandberg syndrome, is an inherited disorder, associated with the progressive accumulation of calcium in the elastic fibers of fibroblast tissue. PXE seems to be a metabolic disease, where a (currently unidentified) molecule loses or changes its function, causing a change in elastic tissue. The most common symptoms are skin lesions (typically around the neck) as well as ocular and cardiovascular manifestations. Since the eyes are usually the first affected organ, most diagnostic methods focus on ocular manifestations like irregularities of the pigments in the macula (which share a similarity to cellulite, hence the name Peur d'orange) or angioid stripes that are visible in the retina. The genesis of the angioid stripes is unclear; the stripes themselves are fractions of the thickened and calcified Bruch's membrane.

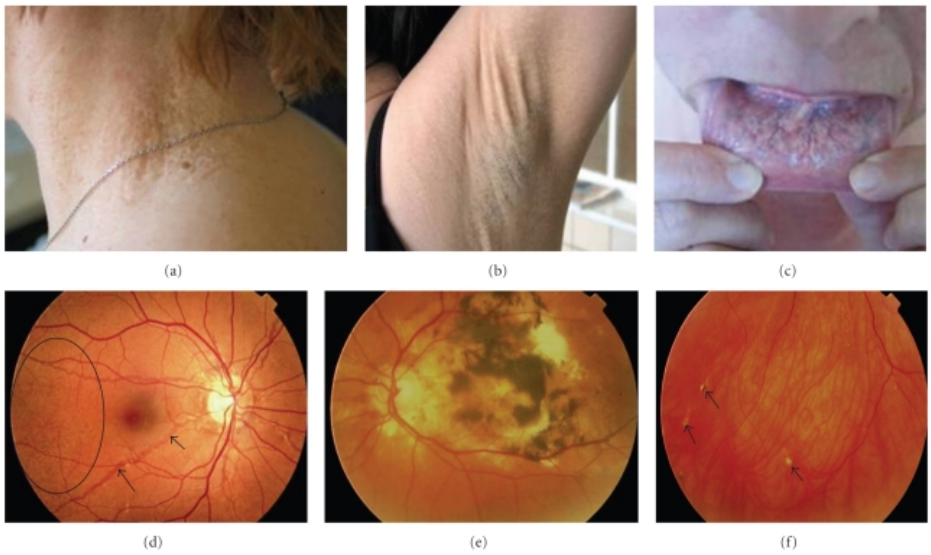


Figure 4.3: Cutaneous and ophthalmological symptoms of PXE. Plaques of papules in the neck region (a), increased skin laxity (b) and mucosal involvement with yeloowish pattern on the inner lip (c). The retinopathy consists of peau d'orange (d, oval), angioid streaks (d, arrowed), retinal hemorrhaging (e). In some cases calcifications of Bruch's membrane can be seen as comets or comet tails (f, arrowed). [**?**]

According to recent studies, PXE is inherited as an autosomal recessive trait, and an association with the ABCC6 gene on chromosome 16p13.1 hast been shown. (ANGABE???) The accumulation of substrate and the calcification of fibers is

caused by mutations within the ABCC6 gene, which lead to reduced or absent transmembraneous transport. Currently, there is no treatment available. Due to a certain variability in phenotypic expression, a correct diagnosis can be difficult. This variability, which occurs even within families also indicates that additional environmental factors like nutrition or hormones might affect the actual phenotype.

# Chapter 5

# Materials and Methods

The work in hand is part of a series of research projects associated with the Herz- und Diabeteszentrum Nordrhein-Westfalen (HDZ NRW) - Universitätsklinikum der Ruhr-Universität Bochum, which also provided the cells used in this experiment. The TMEM43 cells have been provided by the Erich und Hanna Klessmann-Institut für Kardiovaskuläre Forschung und Entwicklung, the PXE cells by the Institut für Laboratoriums- und Transfusionsmedizin. Since these genetic defects affect all the cells in a patient and the extraction of heart cells via biopsy is rather invasive, the experiments were conducted with skin fibroblasts. The cells were extracted from patients using a procedure called XXXXXXX, which is basically piercing the skin. All further handling took place in-house.

## 5.1 Sample Creation

### Cell Culture

The cells were stored and cultivated in an incubator at 37 degrees Celsius and 5 % $CO_2$ concentration. The composition of the culture medium that was used to facilitate the cell growth can be found in Table 5.1.

The culture media used for both cell types were identical except one ingredient: The so-called red DMEM additionally contains Phenol-Red, a dye that serves as a pH indicator. The yellow DMEM does not contain a pH indicator. The addition of Phenol Red is not without problems; in the past, certain properties have been discussed that might have an effect similar to growth hormones [PAPER??????]

Table 5.1: Composition of the culture medium

| Component | Details | Manufacturer | Amount |
|---|---|---|---|
| DMEM | +L-Glutamin<br>+4,5 g/L Glucose<br>+25 mM HEPES | Gibco | 500mL |
| FCS | Fetal Calf Serum | PAA | 50mL (10%) |
| 100x MEM NEAA | non-essential amino acids | Sigma | 5mL (1%) |
| Pen/Strep | 10000U/mL Penicillin<br>1000$\mu$g/mL Streptomycin | Biochrom | 5mL (1%) |
| 2-Mercaptoethanol | | Fluka | 450 $\mu$L |

## 5.2 Cell cultivation & preparation

During the cell cultivation, the cells become confluent; meaning the cells will start to adhere to the agarose surface layer of the culture flask. The progress is monitored via microscope typically every other day. To maintain their proliferative phenotype and to prevent the formation of multilayers of cells, which could make the separation into single cells later on difficult, the cells have to be periodically separated from the surface (passaged).
The harvesting of the cells from the from the bottom surface of the flask is realized by using an enzyme called trypsin, which cleaves certain proteins bonding the cultured cells to the agarose layer. A small amount (0,5-1 mL) will be dripped on the bottom surface and has to interact for a certain amount of time. The enzyme also attacks the cell envelope, so the exact duration is a critical factor in this process. It is somewhat difficult to predict the exact behavior of the cells; it depends heavily on the type of cells used. Some phenotypes are more prone to aggregation even an this stage, others have to be manually removed from the surface using a so-called "policeman" (scraper rod with rubber or Teflon tip). Typically, an empirical value is used, which is determined by optical control (little flakes appear to be visible at the surface once the cells start to detach; they form a white movable layer). The initial value used in the experiments was 5 minutes. Once a sufficient amount of cells are detached from the surface, the reaction process has to be stopped by using a buffer, and the resulting liquid will be removed from the flask. A portion of the resulting fluid will be passed back into the flask with some additional fresh culture medium, allowing the contained cells to resettle on the surface. The remaining fluid is usually discarded, or in this case it is the source material for the extraction of the cells used for the measurements.
The cell concentration recommended by the manufacturer of the stretcher setup is 1-1.5 million cells per mL. This allows for a reasonably fast processing speed during the experiments. The concentration found in the resulting liquid directly after trypsinization was approx. 300000 cells per mL (the concentration was determined several times using a hemocytometer (Neubauer counting chamber)). Therefore, the concentration after trypsinization has to be increased by centrifuging. This step is somewhat challenging, since cells are prone to aggregate on the bottom of the flask (so-called pellets) when being subjected to increased gravitational forces, which would lead to a clogging of the microfluidic path when being inserted into the stretching setup. The g-forces typically used in the protocols are too high, since the protocols are written to facilitate re-suspension of cells, where aggregation is not an issue. Several test runs resulted in a value of 9.5g for centrifugation, more than ten times lower than specified in the protocols. Although, even lower g-forces would most likely be possible.
During the first measurements, several incidents regarding cell aggregation and eventual clogging in the measurement chamber occurred. To prevent this, a change of suspension medium from DMEM to PBS (Phosphate-buffered saline) was implemented. In theory, DMEM should stimulate the cells to consolidate, so the usage of PBS could circumvent that. A disadvantage could be a diminished lifespan of the cells, which was not examined separately. This implies an additional instance of centrifugation in the preparation protocol, which seems applicable given the continuously increased efficiency of the measurements.
Based on the previous explications, the exact protocol for the cell preparation had to be altered several times during the duration of the experiments to for the updated requirements (high cell count, no clustering, different suspension medium). The final protocol used is as follows:

- 1

- 2
- Use orbital shaker or vortex shaker (depending on the size of the flask) to make sure that the solution is thoroughly mixed

**Cell staining**

**"Soft" Cell Preparation**

Since the preparation of cells can be somewhat difficult, there is a certain need for techniques that will achieve the required suspension properties (high cell count, no clustering, different suspension medium). This paragraph serves as a resource for several ideas on how to achieve these properties of the cell suspension:

- cultivation of the cells in the desired concentration
- Using very low g-forces: Necessary to prevent the formation or increase of pellets in the Eppendorf tubes used in the centrifuge
- mechanical filtering

## 5.3 Experimental setup

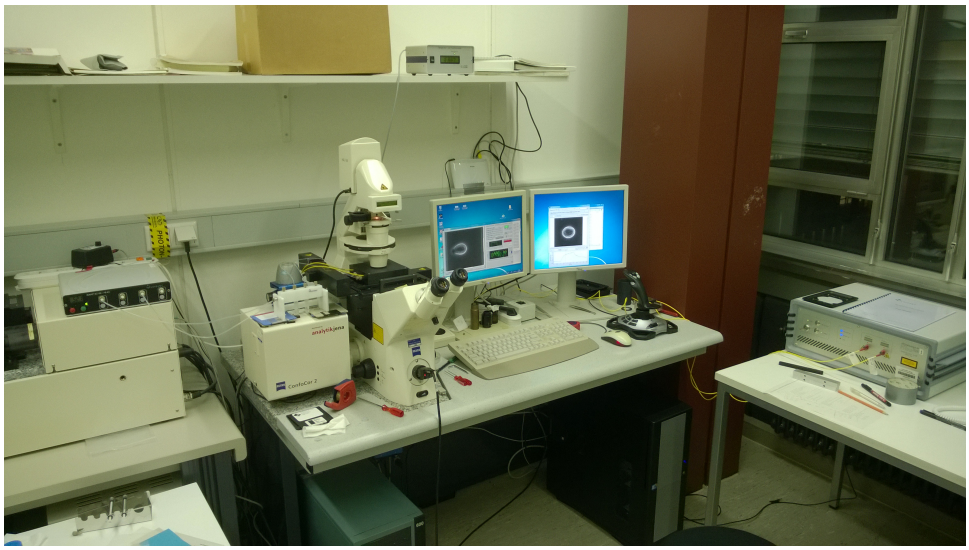

Figure 5.1: Setup

The experimental setup consists of:

- Microscope Zeiss Axiovert 200, equipped with a LD Plan-Neofluar 63x/0.75 Corr Ph2 and a Ximea xiQ camera
- Measurement chamber
- Fluigent MFCS-4C incl. a separate retainer for the sample tubes and the waste tube
- FiboTec 2x2W singlemode laser with fiber optic coupling

- PC with Software to control all the components, allowing for video-based automated measurement of the cell deformation
- A sensor to measure the temperature near the measurement chamber

## 5.4 Software

## 5.5 Measurement Sequence

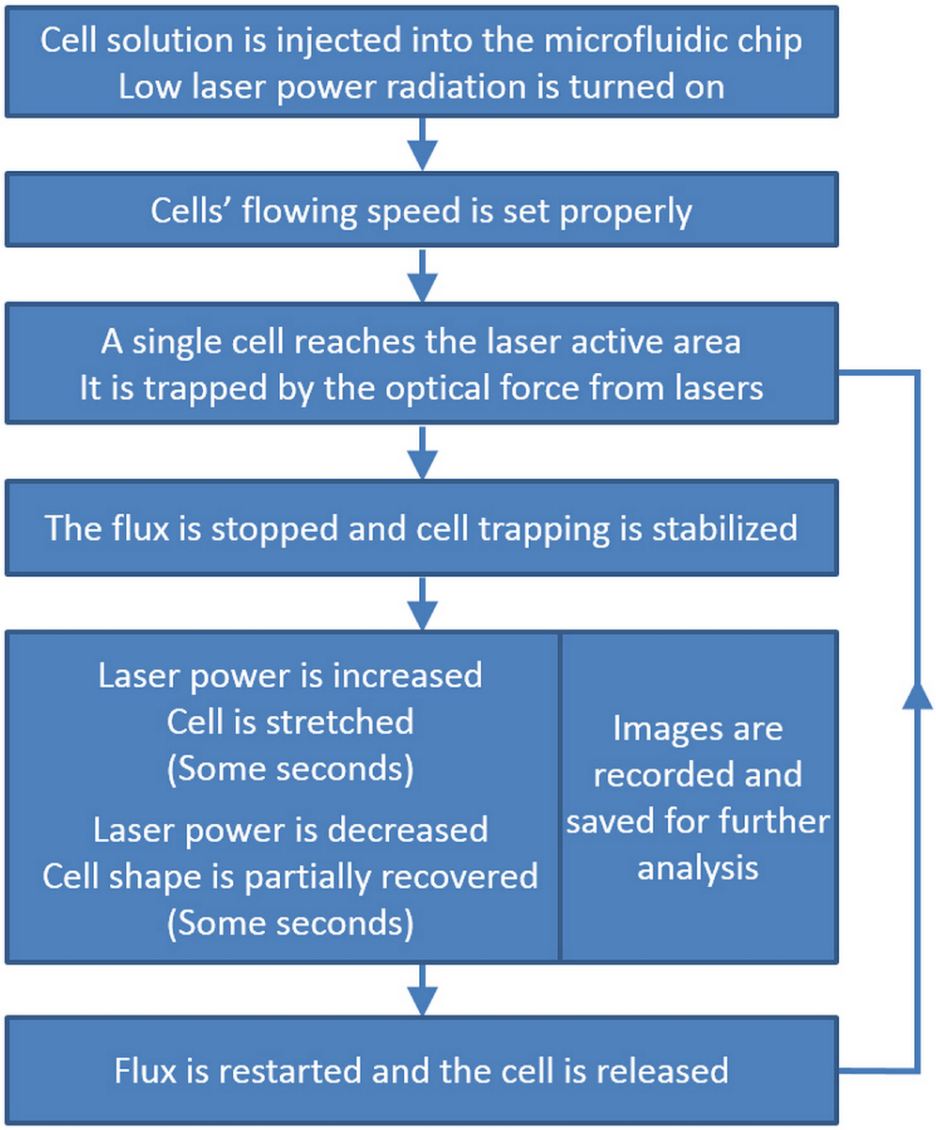


Figure 5.2: Flow chart of continuous cell stretching procedure [**?**]

# Chapter 6

# Results

This is an outline of the scale and efficiency of the performed measurements.
A comparison with literature values is basically not possible, since the mechanical behavior of cell systems in suspension has not been studied extensively yet.

| cell type | | cell line | |
|---|---|---|---|
| TMEM43 | Arya DMEM | Cersei DMEM | - |
| | Arya PBS | - | Tyrion PBS (x2) |
| PXE | - | P9 DMEM (x2) | |
| | P8 PBS (x2) | P9 PBS | |

Table 6.1: outline of measured cell lines

This overview shows several things:

- The change of suspension media from DMEM to PBS did not have a significant increase in measurement efficiency
- The first measurements feature a lower cell count due to technical difficulties (cell aggregates blockages of the microfluidic chamber)
- Bla

The analysis will put an emphasis on the following questions:

- Comparison of two measurements under identical conditions to determine the influence of the room temperature: (Tyrion(PBS), P8(PBS), P9(DMEM))
- Comparison of two cell lines of the same type in different medium to determine the influence of the medium: (Arya und P9, jeweils DMEM vs. PBS)
- Comparison of two cell lines of the same type to determine the "'relative"' elasticity: (Tyrion vs. Arya vs. Cersei, P8 vs. P9)

During measurements, several problems did occur. The most severe relates to the cell line Cersei of the TMEM cells, in which the handling proved to be extremely difficult. Cell aggregates were visible in the sample tube after the preparation, which clogged the feed line to the measurement chamber shortly after beginning. At the second attempt, the feed line was clogged already at the beginning of measurement. During the preparation of the third attempt, mold was discovered in the culture

| cell line | measured | not recognized | detection efficiency [%] | discarded | considered | efficiency [%] |
|---|---|---|---|---|---|---|
| 06.11 Arya (DMEM) | 556 | 213 | 61.7 | 124 | 219 | 39.4 |
| 13.11 P9 (DMEM) | 363 | 155 | 57.3 | 68 | 140 | 38.6 |
| 16.11 Cersei (DMEM) | 71 | 21 | 70.4 | 18 | 32 | 45.1 |
| 18.11 Arya (PBS) | 897 | 488 | 45.6 | 179 | 230 | 25.6 |
| 19.11 P9 (DMEM) | 933 | 253 | 72.9 | 220 | 460 | 49.3 |
| 20.11 P8 (PBS) | 716 | 174 | 75.7 | 215 | 327 | 45.7 |
| 21.11 Tyrion (PBS) | 1509 | 423 | 72.0 | 441 | 645 | 42.7 |
| 24.11 P9 (PBS) | 1557 | 360 | 76.9 | 503 | 694 | 44.6 |
| 25.11 P8 (PBS) | 881 | 165 | 81.3 | 297 | 419 | 47.6 |
| 30.11 Tyrion (PBS) | 1224 | 599 | 51.1 | 262 | 363 | 29.7 |
| total | 8707 | 2762 | 66.5 | 2416 | 3529 | 40.8 |

flask, which is why the cell line was destroyed to prevent further infestation. Because of this, only a single data set with 32 considered measurements is available for Cersei.

The original plan was to divide the measurement period in several intervals and compare with the corresponding temperature curves, so as to examine a correlation between the temperature difference and the long axis deformation. However, this approach has relatively little significance due to the temporally highly heterogeneous throughput. In the measurement P8 (25.11), given a subdivision of the temperature profile into three intervals of two hours each, only 34 and 46 events would fall in the first two intervals, whereas the third interval would contain 339 events. A check for other possibly eligible measurements showed a similar pattern with a severe inequality regarding throughput. Because of these reasons, this part of the analysis had to be canceled. The exact reason for the unequal distribution of counts is not entirely clear; difficulties in handling the preparation process and the initial start of the measurement process are the most likely reasons. On the other hand, whether the cell counts have to be evenly distributed over the course of the measurement is also not necessarily clear.

## 6.1 Identical Conditions

### P9 vs. P9

As shown in table 6.1, the mean values for the long axis deformation are virtually identical, the difference of 1.1% is within the statistical noise. The temperature curve shows that the conditions were identical during the the main duration of the measurement. This implies that the setup provides constant readings at constant environmental parameters.

Table 6.2: P9 vs. P9

| | P9(13.11) | P9(19.11) |
|---|---|---|
| LA_Def [%] | 3.2799 | 3.2432 |
| SA_Def [%] | -0.45314 | -0.40831 |
| Relaxation [%] | 55.8347 | 46.0554 |
| Mean Area [Px] | 19011.2724 | 19219.6144 |
| Cell Count | 140 | 460 |

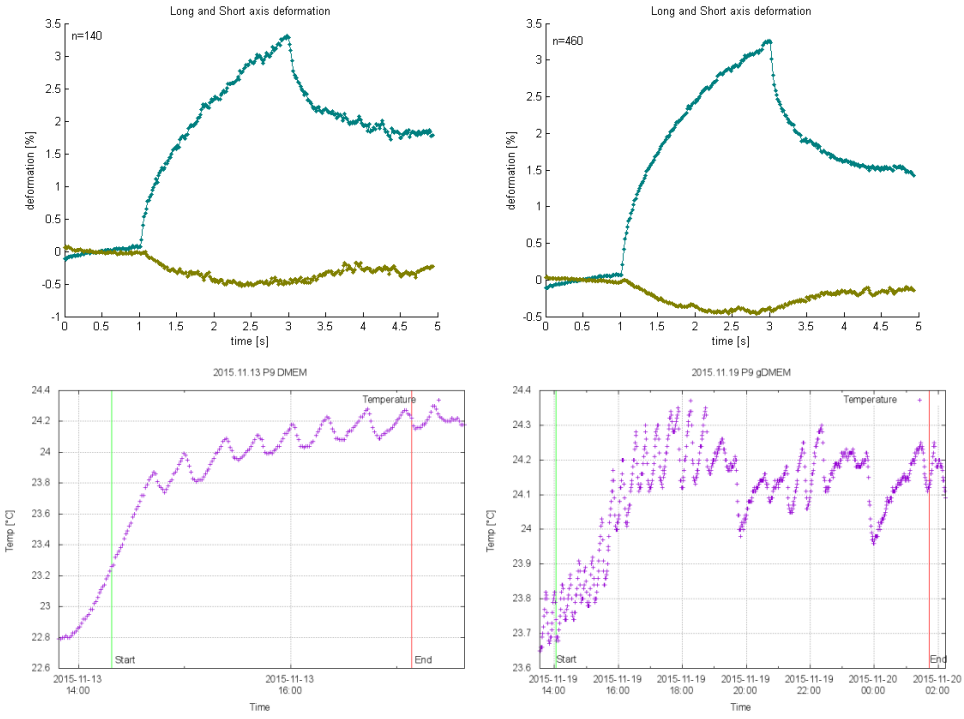


Figure 6.1: overview P9 vs. P9 incl. temperature measurement

### P8 vs. self

A comparison of these two measurements shows a difference of 10.4% in long axis deformation. This seems somewhat high for two measurements under identical conditions; however, the table also shows a fairly significant difference in cell size (mean area). This could indicate a non-optimal focal plane, which would result in smaller images. The temperature curves are somewhat similar in their final temperature value.

Table 6.3: P8 vs. P8

| | P8(20.11) | P8(25.11) |
|---|---|---|
| LA_Def [%] | 2.0425 | 1.849 |
| SA_Def [%] | -0.65706 | -0.55111 |
| Relaxation [%] | 42.2615 | 37.303 |
| Mean Area [Px] | 16469.5847 | 20577.5756 |
| Cell Count | 327 | 419 |

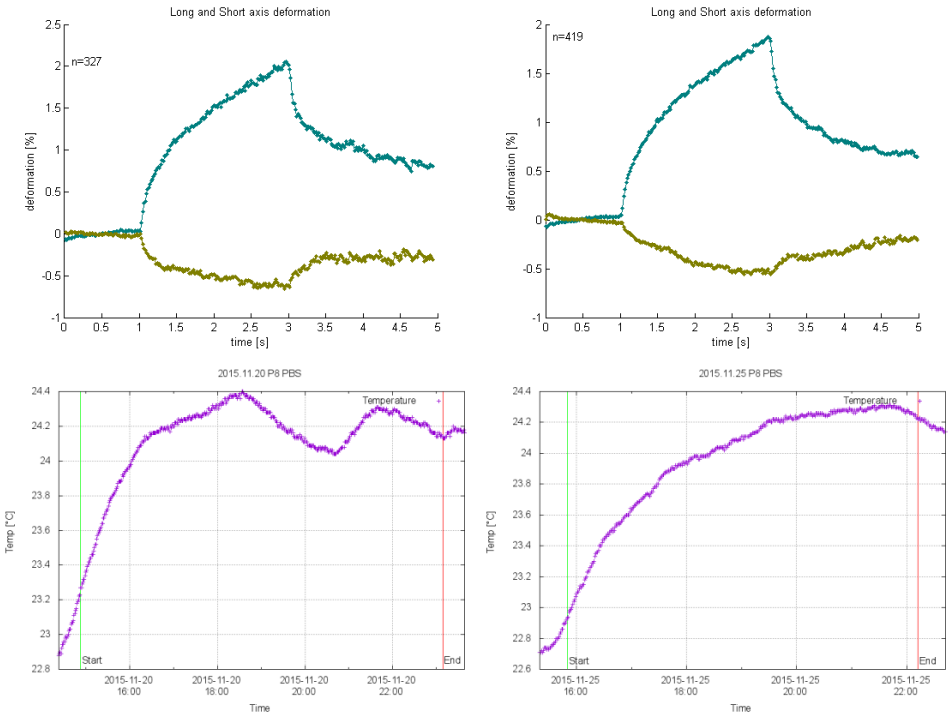


Figure 6.2: Overview P8 vs. P8 incl. temperature measurement

### Tyrion vs. self

These two measurement also show a slightly larger difference in long axis deformation than expected (11, 1%). This measurement also shows a significant difference in cell size (mean area), which draws the same conclusion as in the previous section (focal plane not optimal). The "plateau" of the temperature curve of Tyrion (30.11) is slightly higher, which could provide a partial explanation for the increased long axis deformation.

Table 6.4: Tyrion vs. Tyrion

| | Tyrion(21.11) | Tyrion(30.11) |
|---|---|---|
| LA_Def [%] | 1.8489 | 2.0543 |
| SA_Def [%] | -0.73414 | -0.65759 |
| Relaxation [%] | 50.1212 | 43.3046 |
| Mean Area [Px] | 24646.5704 | 28311.7436 |
| Cell Count | 645 | 363 |

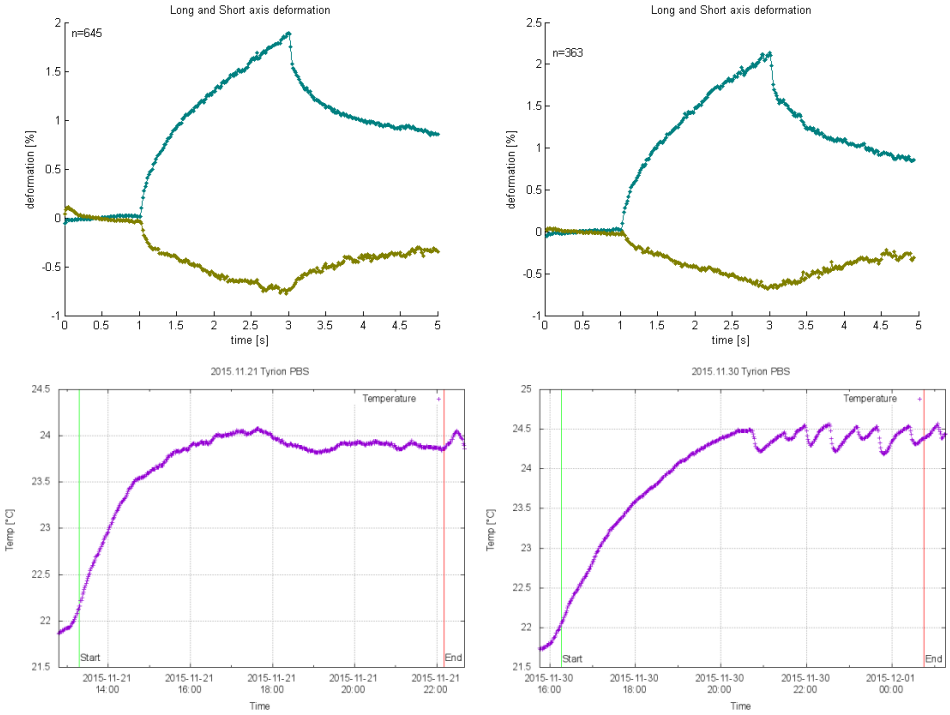


Figure 6.3: Overview Tyrion vs. Tyrion incl. temperature measurement

## 6.2 Different suspension media

### P9(DMEM) vs. P9(PBS)

Fluctuation 31, 7%, P9 (19.11) deviation 5%, P9 (24.11) deviation 5%

Table 6.5: P9(DMEM) vs. P9(PBS)

| | P9(19.11) | P9(24.11) |
|---|---|---|
| LA_Def [%] | 3.2432 | 2.4633 |
| SA_Def [%] | -0.40831 | -0.63903 |
| Relaxation [%] | 46.0554 | 52.6861 |
| Mean Area [Px] | 19219.6144 | 28260.5371 |
| Cell Count | 460 | 694 |

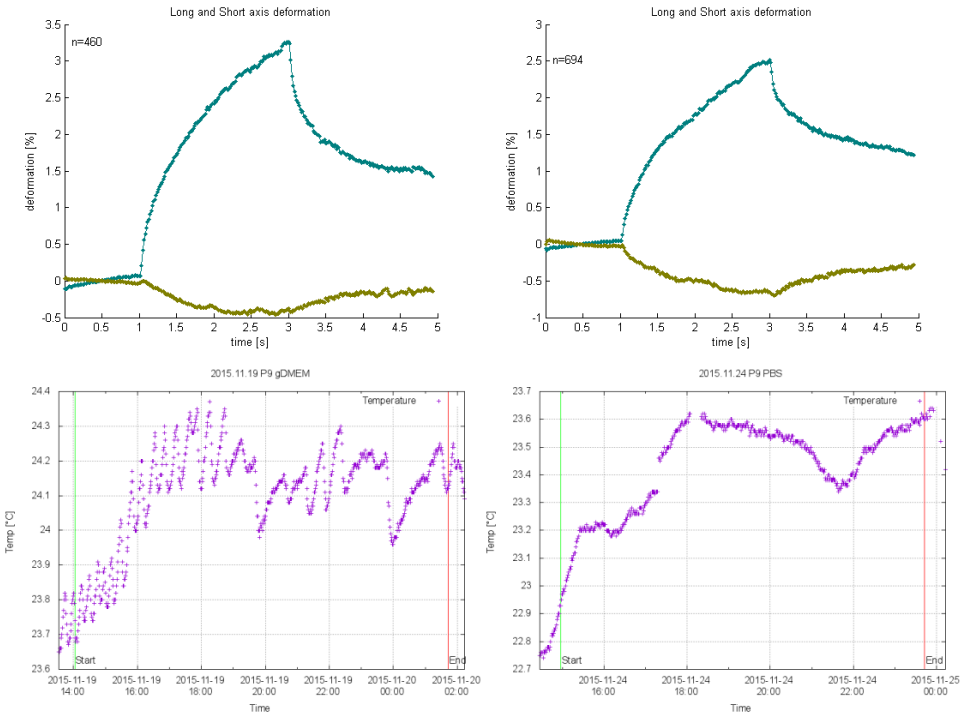


Figure 6.4: Overview P9(gDMEM) vs. P9(PBS) incl. temperature measurement

### Arya(DMEM) vs. Arya(PBS)

Probably the most surprising result of this work is the behavior of the cell line Arya in different suspension media. A comparison of the elasticity curves shows a comparatively viscose behavior (linear slope, the curve remains at a near constant level after the stretch impulse returns to its initial value) for Arya in DMEM suspension, whereas the same cell line in PBS suspension shows a "more" viscoelastic behavior. This observation has to be taken somewhat lightly: The slope of both curves is rather similar, while the decline of the curve in Arya (PBS) shares a resemblance with the other curves that behave similar to the standard linear model. In this regard, it does not follow the "typical" viscoelastic model. The long axis deformation however differs greatly, with a difference of $170,4\%$.
The cell size also differs significantly, although this is somewhat expected, since a change in suspension media is very likely to have an influence of the cell size.

Table 6.6: (Arya(DMEM) vs. Arya(PBS)

| | Arya(06.11) | Arya(18.11) |
|---|---|---|
| LA_Def [%] | 4.4155 | 1.6328 |
| SA_Def [%] | -1.7857 | -0.7346 |
| Relaxation [%] | 89.6232 | 62.0692 |
| Mean Area [Px] | 22071.7893 | 28202.4507 |
| Cell Count | 219 | 230 |

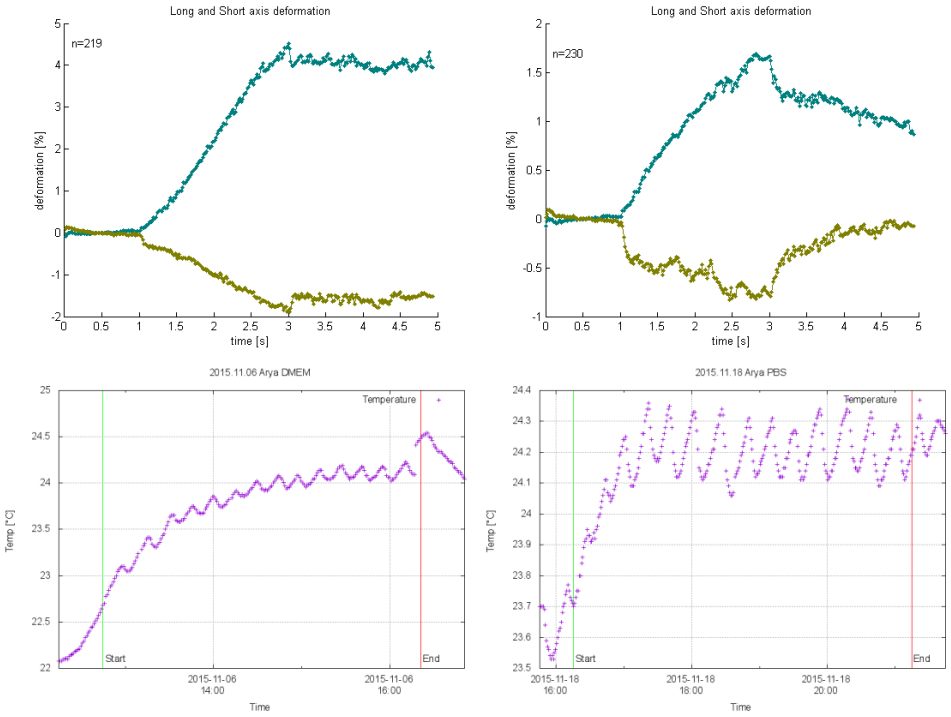


Figure 6.5: Overview Arya(DMEM) vs. Arya(PBS) incl. temperature measurement

### Conclusion

The main finding in the analysis of these two cases is the strong influence of the chosen suspension medium to the long axis deformation. Concerning the short axis deformation, the current data is ambiguous: Tn the cell line P9, the usage of DMEM appears to lower the short axis deformation, whereas the the cell line Arya behaves conversely.

## 6.3 Classification

The data present is sufficient for the classification of the PXE cells. With the ARVC cells, the situation is somewhat complicated. The three cell lines were not measured using the same suspension medium, therefore a direct comparison is difficult. However, it is still possible to make a qualitative statement and ultimately to identify the affiliation of the cell lines.

### Tyrion(PBS) vs. Arya(PBS)

A significant difference in long axis deformation is visible (13, 2%), whereas the short axis deformation is nearly identical. The temperature during the measurement of Arya(18.11) was slightly higher than in the other cell line, and the long acis deformation was even higher during the other instance (Tyrion(30.11)). In this respect, one can assume that the classification "Tyrion has a higher elasticity than Arya" is correct.

Table 6.7: Tyrion(PBS) vs. Arya(PBS)

| | Tyrion(21.11) | Arya(18.11) |
|---|---|---|
| LA_Def [%] | 1.8489 | 1.6328 |
| SA_Def [%] | -0.73414 | -0.7346 |
| Relaxation [%] | 50.1212 | 62.0692 |
| Mean Area [Px] | 24646.5704 | 28202.4507 |
| Cell Count | 645 | 230 |

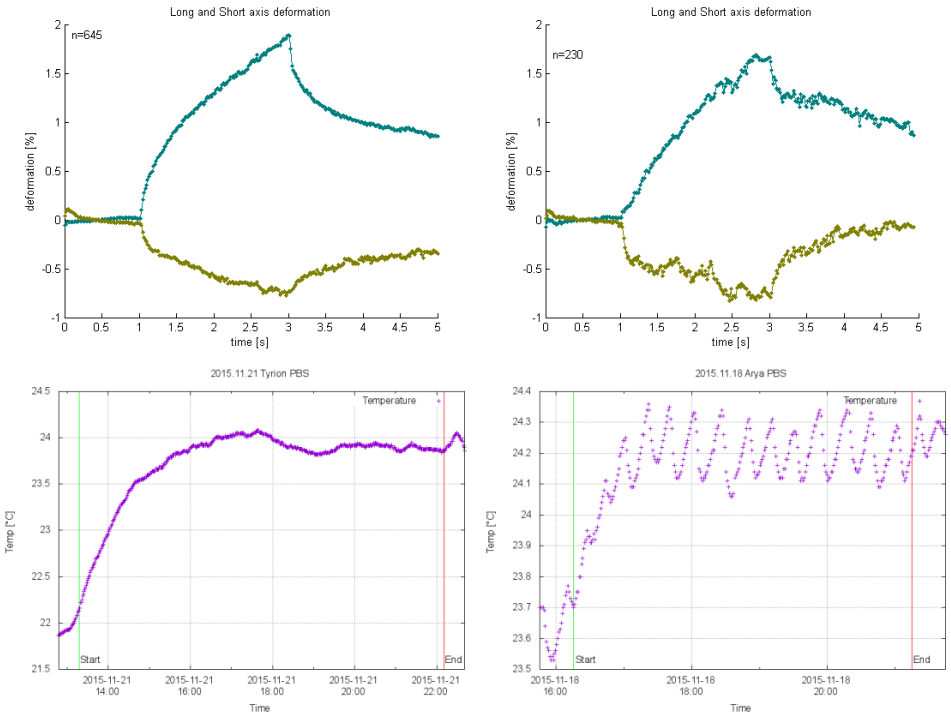


Figure 6.6: Overview Tyrion(PBS) vs. Arya(PBS) incl. temperature measurement

**Arya(DMEM) vs. Cersei(DMEM)**

Table 6.8: (Arya(DMEM) vs. Cersei(DMEM)

| | Arya(06.11) | Cersei(16.11) |
|---|---|---|
| LA_Def [%] | 4.4155 | 2.0115 |
| SA_Def [%] | -1.7857 | -1.1994 |
| Relaxation [%] | 89.6232 | 25.6628 |
| Mean Area [Px] | 22071.7893 | 24098.4047 |
| Cell Count | 219 | 32 |

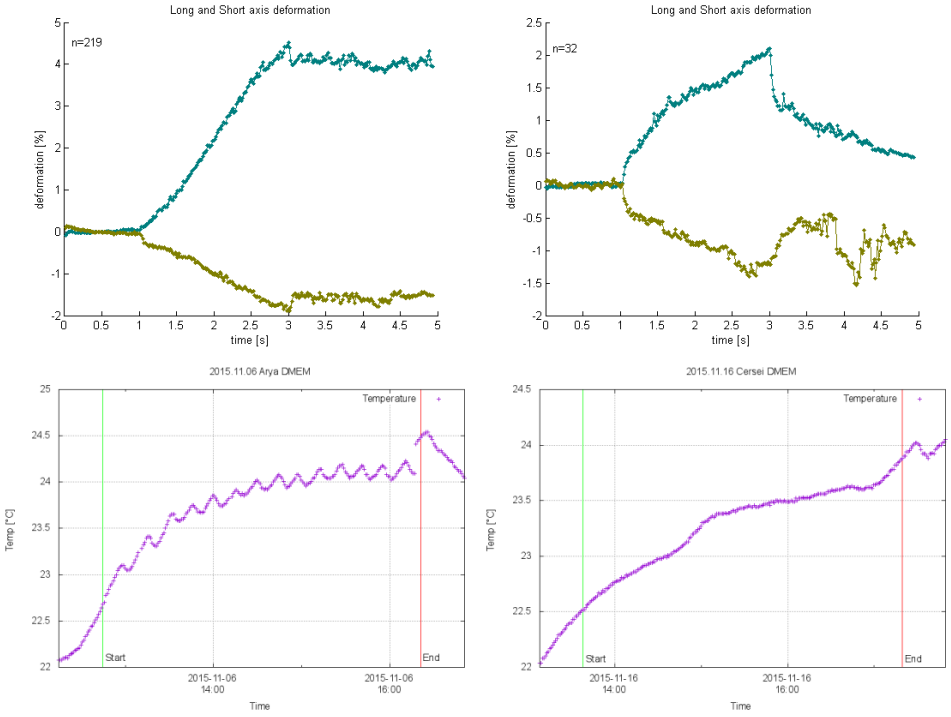


Figure 6.7: Overview Arya vs. Cersei (DMEM) incl. temperature measurement

The difference in long axis deformation between the two groups is $119,5\%$, which allows an easy differentiation. Finally, this table shows the measurements of the ARVC cell line:

Table 6.9: Overview ARVC Cells

| | Tyrion | Arya | Cersei |
|---|---|---|---|
| PBS | $1.84 \pm 5\%$ | $1.63 \pm 2\%$ | |
| DMEM | | $4.42 \pm 10\%$ | $2.01 \pm 15\%$ |

The biggest cause for uncertainty is the exact categorization of the cell line Arya. Due to the large difference in the elasticity compared to Cersei, it can be concluded that Cersei is the abnormal cell line, and both Arya and Tyrion are the "healthy" ones, since the respective long axis deformation values are close $(13,2\%)$. However, due to the very low number of cell counts during the measurement of Cersei, it is somewhat questionable if the measurement can be considered representative.

### P8(PBS) vs. P9(PBS)

As seen in paragraph 5.1, identifying the causes for deviation in two separate measurements under seemingly identical environmental conditions is challenging. The choice seems to be somewhat arbitrary. Due to the larger number of cell counts, the measurement P8(25.11) was used in this analysis.
The difference of $20,6\%$ (or $33,2\%$ in P9(24.11)) for the long axis deformation is significant enough to warrant a reliable differentiation. Since the main symptom of PXE is calcification of fibers, which would suggest a decreased elasticity, the data present implies that P8 are the PXE cells and P9 the control group.

Table 6.10: P8(PBS) vs. P9(PBS)

| | P8(20.11) | P8(25.11) | P9(24.11) |
|---|---|---|---|
| LA_Def [%] | 2.0425 | 1.849 | 2.4633 |
| SA_Def [%] | -0.65706 | -0.55111 | -0.63903 |
| Relaxation [%] | 42.2615 | 37.303 | 52.6861 |
| Mean Area [Px] | 16469.5847 | 20577.5756 | 28260.5371 |
| Cell Count | 327 | 419 | 694 |

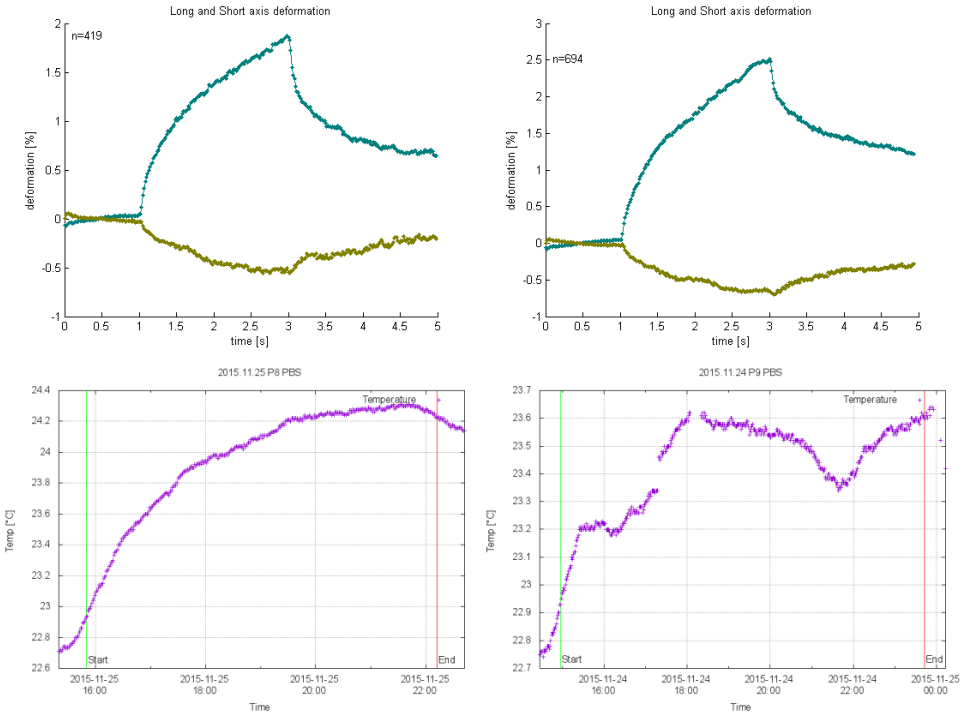


Figure 6.8: Overview P8(PBS) vs. P9(PBS) incl. temperature measurement

## 6.4 Specific long axis deformation interval for healthy cells

The data presented leads to the conclusion that a specific long axis deformation interval for healthy cells most likely does exist, ranging from XXXX to XXXX %.

Table 6.11: Healthy Cells

| Cell Line | DMEM | PBS |
|---|---|---|
| Cersei | 2.01 (16.11) | - |
| Arya | 4.41 (6.11) | 1.63 (18.11) |
| Tyrion | - | 1.85 (21.11) |
| | | 2.05 (30.11) |
| P9 | 3.28 (13.11) | 2.46 (24.11) |
| | 3.24 (19.11) | - |
| P8 | - | 2.04 (20.11) |
| | | 1.85 (25.11) |

Table 6.12: Long Axis Deformation Median [%]

| Cell Line | DMEM | PBS |
|---|---|---|
| PXE | 3.26 | 2.46 |
| Control3 | - | 1.95 |

# Chapter 7

# Conclusion

More than 8700 measurements taken, detection rate of 68.5% (40.8% were used for the analysis). Long axis deformation differs significantly, depending on the used suspension medium. The control of environmental temperature is neccessary. A specific long axis deformation interval for healthy cells most likely does exist. The TMEM43 cells are significantly stiffer than control cells (194%, DMEM). Unlike indicated in previous measurements [MASTERARBEIT JAY], PXE cells show a larger long axis deformation than control cells (26,2%, PBS).
Since the mechanical properties of cell are highly dependent on the cell culture protocol and the extraction process, a coherent approach is absolutely crucial. The present results are highly promising and could provide a basis for further research regarding the question of the usage of mechanical properties of cells as an indicator for the prevalence of certain diseases like ARVC or PXE.

# Bibliography

[1] J. Guck, R. Ananthakrishnan, H. Mahmood, T. J. Moon, C. C. Cunningham, and J. Käs, "The optical stretcher: A novel laser tool to micromanipulate cells," *Biophysical Journal*, vol. 81, no. 2, pp. 767 – 784, 2001.

[2] F. Lautenschläger, S. Paschke, S. Schinkinger, A. Bruel, M. Beil, and J. Guck, "The regulatory role of cell mechanics for migration of differentiating myeloid cells," *Proceedings of the National Academy of Sciences*, vol. 106, no. 37, pp. 15696–15701, 2009.

[3] S. Ostermann, M. Sonnleitner, and H. Ritsch, "Scattering approach to two-colour light forces and self-ordering of polarizable particles," *New Journal of Physics*, vol. 16, no. 4, p. 043017, 2014.